Journal of Biomechanics 44 (2011) 995–1000

Contents lists available at ScienceDirect

Journal of Biomechanics

journal homepage: www.elsevier.com/locate/jbiomech
www.JBiomech.com

In vivo kinematics of two-component total ankle arthroplasty during non-weightbearing and weightbearing dorsiflexion/plantarflexion

Satoshi Yamaguchi [a,b,*], Yasuhito Tanaka [a], Shinichi Kosugi [a], Yoshinori Takakura [a], Takahisa Sasho [b], Scott A. Banks [c]

[a] Department of Orthopaedic Surgery, Nara Medical University, Kashihara, Nara 634-8521, Japan
[b] Department of Orthopaedic Surgery, Graduate School of Medicine, Chiba University, Chiba 260-8670, Japan
[c] Department of Mechanical and Aerospace Engineering, University of Florida, Gainesville, FL 32611, USA

ARTICLE INFO

Article history:
Accepted 19 February 2011

Keywords:
Total ankle arthroplasty
Ankle joint
In vivo kinematics
Radiography
3D–2D model-image registration

ABSTRACT

Relatively high rates of loosening and implant failure have been reported after total ankle arthroplasty, especially in first and second generation implants. Abnormal kinematics and incongruency of the articular surface may cause increased loads applied to the implant with concomitant polyethylene wear, resulting in loosening and implant failure. The purpose of this study was to measure three-dimensional kinematics of two-component total ankle arthroplasty during non-weightbearing and weightbearing activities, and to investigate incongruency of the articular surfaces during these activities. Forty-seven patients with a mean age of 71 years were enrolled. Radiographs were taken at non-weightbearing maximal dorsiflexion and plantarflexion, and weightbearing maximal dorsiflexion, plantarflexion, and neutral position. 3D–2D model-image registration was performed using the radiographs and the three-dimensional implant models, and three-dimensional joint angles were determined. The implanted ankles showed $18.1 \pm 8.6^\circ$ (mean $\pm$ standard deviation) of plantarflexion, $0.1 \pm 0.7^\circ$ of inversion, $1.2 \pm 2.0^\circ$ of internal rotation, and 0.8 ± 0.6 mm of posterior translation of the talar component in the non-weightbearing activity, and $17.8 \pm 7.5^\circ$ of plantarflexion, $0.4 \pm 0.5^\circ$ of inversion, $1.8 \pm 2.0^\circ$ of internal rotation, and 0.7 ± 0.5 mm of posterior translation in the weightbearing activity. There were no significant differences between the non-weightbearing and weightbearing kinematics except for the plantarflexion angle. Incongruency of the articular surface occurred in more than 75% of the ankles. Our observations will provide useful data against which kinematics of other implant designs, such as three-component total ankle arthroplasty, can be compared.

1. Introduction

Total ankle arthroplasty is a treatment of choice for end-stage arthritis of the ankle. After disappointing failure rates of the first generation total ankle arthroplasties in the 1970s (Saltzman, 1999; Gougoulias et al., 2009; Bonasia et al., 2010), the second generation implants were developed with improved designs and fixation methods. These implants have been an increasingly popular alternative to ankle arthrodesis in the last decade (Saltzman et al., 2000). The second generation total ankle arthroplasties include two categories (Lewis, 2004): the two-component type consisting of a talar component and a tibial component with the polyethylene insert fixed with the tibial component, and the three-component type consisting of a mobile bearing insert between the components. Although encouraging short- and mid-term clinical outcomes and low revision rates have been reported using these implants, survivorship still is not comparable to total knee and hip arthroplasties, primarily due to implant loosening and subsidence (Michael et al., 2008).

A better understanding of total ankle arthroplasty kinematics is critical to improve operative techniques, prosthetic designs, and clinical outcomes. For example, kinematic analyses provide quantitative in vivo information to determine if an implant operates in accordance with its design objectives (Leardini et al., 2004). Moreover, abnormal kinematics and incongruency of the articular surface may cause increased contact pressure applied to the implant as shown in biomechanical in-vitro studies (Tochigi et al., 2005; Espinosa et al., 2010; Fukuda et al., 2010). This may result in pathologically increased polyethylene wear leading to component loosening and implant failure (Wood et al., 2009). Several studies have reported in vivo three-dimensional kinematics during the stance phase of walking (Conti et al., 2006; Leszko et al., 2008) and ankle dorsiflexion–plantarflexion

* Corresponding author at: Department of Orthopaedic Surgery, Graduate School of Medicine, Chiba University, Chiba 260-8670, Japan. Tel.: +81 43 226 2116; fax: +81 43 226 2117.
E-mail address: y-satoshi@mvb.biglobe.ne.jp (S. Yamaguchi).

0021-9290/$ - see front matter © 2011 Elsevier Ltd. All rights reserved.
doi:10.1016/j.jbiomech.2011.02.078

(Komistek et al., 2000), but the numbers of the patients were relatively small, and incongruency of the articular surface was not fully investigated.

Additionally, understanding the difference between non-weightbearing kinematics and weightbearing kinematics is clinically important because recreating weightbearing activities is difficult during total ankle arthroplasty surgery, and therefore surgeons need to estimate weightbearing kinematics from the intraoperative non-weightbearing condition. Yamaguchi et al. (2009) reported weightbearing ankle kinematics are significantly different from the non-weightbearing kinematics in vivo, and this difference occurs possibly because the ankle kinematics are mainly determined by the tension of the surrounding ligaments in non-weightbearing activities (Leardini, 2001), while in weightbearing activities they are regulated by the articular surface geometry (Tochigi et al., 2006).

We have used the revised version of the TNK Ankle™ (Japan Medical Materials, Osaka, Japan) since 1990 (Fig. 1), and have reported good clinical results (Takakura et al., 2004) comparable to other second generation total ankle arthroplasty designs (Buechel et al., 2004; Claridge and Sagherian, 2009; Wood et al., 2009; Gougoulias et al., 2010). Results have been less favorable in patients with rheumatoid arthritis than in patients with osteoarthritis (Nagashima et al., 2004; Takakura et al., 2004). The TNK ankle is a two-component alumina ceramic prosthesis coated with beads and hydroxyapatite, and a high-density polyethylene insert is fixed on the tibial component. It has cylindrical joint surfaces, and the diameter of the talar surface is slightly smaller than that of the tibial surface, allowing the talar component to slide and rotate in addition to dorsiflexion/plantarflexion. Other features include the medial facet to sustain increased medial loads in ankles with primary varus osteoarthritic deformity, and the use of tissue engineered bone mounted on the upper surface of the tibial component to enhance bonding between the bone and implant (Tohma et al., 2006).

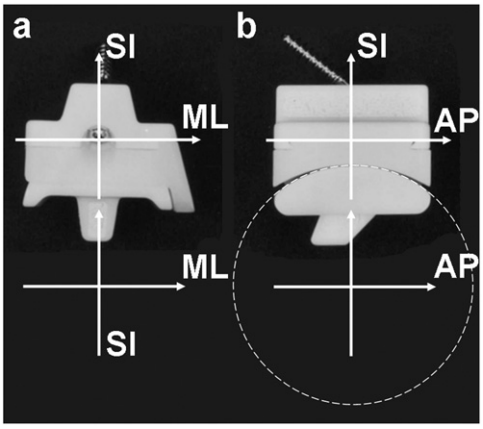

Fig. 1. TNK ankle and the coordinate system of the each component. (a) anterior view and (b) lateral view of the right ankle. AP: anteroposterior axis; SI: superoinferior axis; and ML: mediolateral axis.

3D–2D model-image registration techniques are widely accepted methods for the accurate measurement of in vivo joint kinematics, (Banks and Hodge, 1996; You et al., 2001; Mahfouz et al., 2003) although few ankle studies have been reported (Yamaguchi et al., 2009). To begin this study, we quantified the accuracy and reproducibility of the 3D–2D model-image registration techniques for the TNK Ankle system. We then measured in vivo kinematics of the TNK Ankles during non-weightbearing and weightbearing dorsiflexion/plantarflexion activities using these techniques. From our clinical experience, we hypothesized: (1) in the non-weightbearing activity, incongruency of the articular surfaces would be observed, and (2) in the weightbearing activity, the loaded articular surfaces would better control motions and reduce the observed surface incongruencies.

2. Methods

2.1. 3D–2D model-image registration

Three-dimensional implant models were obtained from the manufacturer, and an anatomic coordinate system was embedded in each implant (Fig. 1). For the tibial component, the mediolateral midline of the inferior surface of the implant was defined as the anteroposterior axis, the anteroposterior midline was defined as the mediolateral axis, and the intersection of the axes was the origin. The superoinferior axis was defined as the cross product of the two other axes. For the talar component, a circle was fitted to its joint surface in the mediolateral center, and the center of the circle was defined as the origin. The perpendicular to the circle, passing though the origin was defined as the mediolateral axis, and the perpendicular to the inferior surface of the implant, passing through the origin was the superoinferior axis. The anteroposterior axis was the cross product of the other two axes.

In vivo three-dimensional position and orientation of each implant were determined from a lateral radiograph of the implant and the implant models using 3D–2D model-image registration techniques, including previously reported techniques, manual matching, and automated matching using nonlinear least-squares minimization techniques (Banks and Hodge, 1996; Moro-oka et al., 2007). The implant model was projected onto the lateral radiographic image of the implant, and its three-dimensional pose was iteratively adjusted to match its silhouette with the silhouette in the radiographic image (Fig. 2a and b). Joint angles were expressed as motion of the talar component relative to the tibial coordinate system, following conventional clinical descriptions of motion. Plantarflexion–dorsiflexion was defined as rotation of the talar component along its mediolateral axis, internal–external rotation was rotation of the talar component about the superoinferior axis of the tibial component, and inversion–eversion was rotation of the talar component along an axis that is mutually perpendicular to the superoinferior axis of the tibial component and mediolateral axis of the talar component using a plantarflexion- internal rotation-inversion sequence.

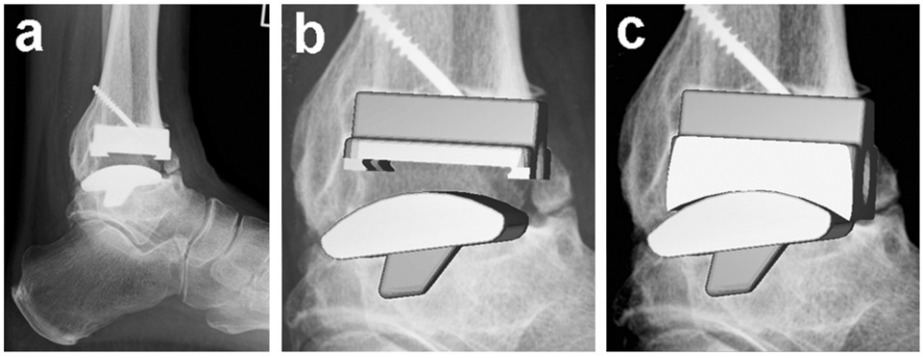

Fig. 2. 3D–2D model-image registration of the implant models. The models were projected onto the radiographic image (a) and their three-dimensional poses were iteratively adjusted to match the radiographic image (b). After 3D–2D model-image registration, the polyethylene insert was projected, and congruency of the joint surface was assessed (c). The medial facet of the implant was eliminated to visualize the joint surface.